

Experimental investigation of muon catalysis of the fusion of deuterium and tritium nuclei

V. M. Bystritskiĭ, V. P. Dzhelepov, Z. V. Ershova, V. G. Zinov, V. K. Kapyshev, S. Sh. Mukhamet-Galeeva, V. S. Nadezhdin, L. A. Rivkis, A. I. Rudenko, V. I. Satarov, N. V. Sergeeva, L. N. Somov, V. A. Stolupin, and V. V. Fil'chenkov

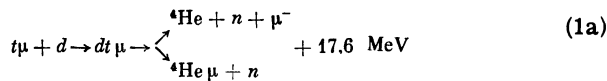
Joint Institute for Nuclear Research
(Submitted 12 December 1980)
Zh. Eksp. Teor. Fiz. 80, 1700-1714 (May 1981)

The yields and temporal distributions of neutrons from the fusion reaction in the $d\bar{t}\mu$ mesomolecule have been measured in experiments with a gas target filled with purified deuterium and tritium at various pressures in a muon beam from the JINR synchrocyclotron. The experiments were carried out at several tritium concentrations in the temperature range from 93 to 613 K. These data have been used to obtain the lower limit of the production rate of $d\bar{t}\mu$ molecules, $\lambda_{d\bar{t}\mu} > 10^8 \text{ sec}^{-1}$, and the rate of muon transfer from deuterium to tritium, $\lambda_{dt} = (2.9 \pm 0.4) \times 10^8 \text{ sec}^{-1}$. The value found for the lower limit of the $d\bar{t}\mu$ -molecule production rate confirms the existence of the theoretically predicted mechanism, at resonance with the $t\mu$ atom energy for the formation of this molecule. The value of the transfer rate λ_{dt} is also in good agreement with the theoretical value.

PACS numbers: 25.30.Ei, 25.10.+s, 36.10.Dr

INTRODUCTION

Although muon catalysis of the reactions of fusion of hydrogen isotope nuclei $p + d$ and $d + d$ was first detected more than twenty years ago¹ and since then has been studied by many experimental groups, the fusion of nuclei from a state of the muonic molecule $d\bar{t}\mu$



(1b)

has not yet been studied.

However, in the last few years there has arisen an urgent need for experiments on process (1) in order to establish the resonance nature of the production of $d\bar{d}\mu$ muonic molecules²⁻⁵ and to check the theoretically predicted⁵ existence of a similar resonance in the cross section for producing the $d\bar{t}\mu$ molecule. The calculations of Ref. 5 carried out on the basis of a study of the resonance mechanism⁴ of muonic-molecule production indicate that the rate of $d\bar{t}\mu$ molecule production can reach values $\lambda_{d\bar{t}\mu}^0 \sim 10^8 \text{ sec}^{-1}$ at the density of liquid hydrogen, that is, it can exceed the muon decay rate $\lambda_0 = 4.55 \times 10^5 \text{ sec}^{-1}$ by more than two orders of magnitude. This means that in a mixture of deuterium and tritium a single muon can successively initiate more than a hundred reactions of the type (1a) during its lifetime.^{5,6} Experimental verification of this conclusion is of considerable interest from the viewpoint of the possibility of using muon catalysis of the reaction $d + t$ for energy production purposes.⁷

The purpose of the present study was to record the reaction (1), measure its yield, and thereby verify the theoretical prediction of a resonance in the cross section for $d\bar{t}\mu$ molecule production. The experiment was designed to use a gas target filled with a $D_2 + T_2$ mixture, which made it possible to carry out measurements in a wide range of target temperatures ($T = 90\text{--}610 \text{ K}$). The Process was recorded by the detection of neutrons of energy 14.1 MeV, produced in the

reaction (1). The preliminary data were published in Ref. 8.

The processes induced by negative muons in a mixture of deuterium and tritium are shown in Fig. 1. When the muons are slowed down $d\mu$ and $t\mu$ atoms are formed at rates $\lambda_d c_d$ and $\lambda_t c_t$, respectively, where λ_a is the rate of hydrogen mesoatom production and c_d and c_t are the relative deuterium and tritium concentrations ($c_d + c_t = 1$). According to Refs. 9 and 10, at a relative hydrogen density $\varphi \geq 10^{-3}$ ($\varphi = \rho/\rho_0$, where ρ is the density of gaseous hydrogen and $\rho_0 = 4.22 \times 10^{22}$ nuclei/cm³ is the density of liquid hydrogen) we have $\lambda_a \gg \lambda_0$. The $d\mu$ atoms can form muonic molecules $d\bar{d}\mu$ or can participate in isotope exchange reactions



which lead to the formation of $t\mu$ atoms with initial energy 19 eV. The calculations of Ref. 11 give the following for the value of the transfer rate:

$$\lambda_{dt}^0 = 1.9 \cdot 10^8 \text{ sec}^{-1} \quad (3)$$

(referred to the density of liquid tritium). The experimental value of λ_{dt} has not yet been determined and must also be found.

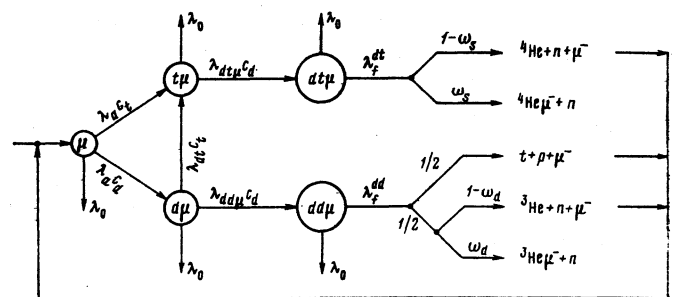


FIG. 1. Processes initiated by negative muons in a mixture of deuterium and tritium.

The $t\mu$ mesoatoms produced as a result of atomic capture of a free muon, or as a result of the charge exchange (2), form $dt\mu$ molecules in collisions with deuterons (rather, with D_2 and DT molecules). The fusion reactions shown in Fig. 1 occur in $dd\mu$ and $dt\mu$ molecules.

Because of the fusion reaction, in most cases a muon is able to free itself and again initiate the processes shown in Fig. 1, but there is a certain probability (ω) for it to become bound to one of the charged reaction products. It is important that the charged systems (${}^4\text{He}\mu^+$ and ${}^3\text{He}\mu^+$) cannot again produce muonic molecules, since if the muon becomes bound to the helium nucleus and does not get "shaken off" as the $(\text{He}\mu)^+$ ion is slowed down, it is knocked out of the succeeding μ catalysis cycles. According to the calculations of Refs. 12 and 13, the probability for the muon to be "shaken off" is $\approx 25\%$.

The calculated production rates of the $dd\mu$, $dt\mu$, and $tt\mu$ molecules, the rates at which the fusion reactions occur in these molecules, and the relative probabilities for the different channels of these reactions are given in Table I. There we give also the experimental values for the production rate of the $dd\mu$ system, the rate of the $d+d$ reaction in this mesomolecule, and the probability for the muon to "stick" to the charged products of this reaction. These characteristics have not yet been experimentally determined in the case of the $dt\mu$ and $tt\mu$ molecules.

The values of $\lambda_{dt\mu}^0$, $\lambda_{dd\mu}^0$, and $\lambda_{tt\mu}^0$ are given for the density of liquid hydrogen $\rho_0 = 4.22 \times 10^{22}$ nuclei/cm³ and can be converted to those for the density of gaseous hydrogen with relative density $\varphi = \rho/\rho_0$ as follows:

$$\lambda_{dt\mu} = \lambda_{dt\mu}^0 \varphi, \quad \lambda_{dd\mu} = \lambda_{dd\mu}^0 \varphi, \quad \lambda_{tt\mu} = \lambda_{tt\mu}^0 \varphi.$$

It can be concluded from the data given in Table I that for the theoretically predicted large values $\lambda_{dt\mu} \gg \lambda_{dd\mu}$, $\lambda_{tt\mu}$ the quantities $\lambda_{dt\mu}$, λ_{dt} , and ω_s determine in the main the efficiency of muon catalysis in a mixture of deuterium and tritium.

The kinetics of mesomolecular processes in a mixture of deuterium and tritium were studied in Ref. 16, where it was shown that at pressures $P = 5-100$ atm

TABLE I. Rates of mesomolecular processes occurring in a mixture of deuterium and tritium and relative probabilities of different fusion reaction channels in mesomolecules.*

Muonic molecule production rates (in units of 10^6 sec^{-1})	Nuclear reaction rates (in units of 10^{10} sec^{-1})		Relative probabilities of fusion reaction channels					
	theory	experiment	theory	experiment	theory	experiment		
$\lambda_{dt\mu}^0$	100 [5]	—	λ_f^{dt}	100 [12, 15]	—	ω_s	0.01 [12, 13, 15]	—
$\lambda_{tt\mu}^0$	3 [14]	—	λ_f^{tt}	10 [15]	—	ω_t	0.1 [13]	—
$\lambda_{dd\mu}^0$	0.8 [5]	0.8 [2, 3]	λ_f^{dd}	10 [15]	$> 2 \cdot 10^{-3}$ [3]	ω_d	0.13 [13, 15]	< 0.13 [2]

* Here the $\lambda_{tt\mu}^0$, λ_f^{tt} , and ω_t denote respectively the production rate of $tt\mu$ muonic molecules, the nuclear reaction rate in this mesomolecule, and the relative probability of the fusion reaction in $tt\mu$ with production of the $({}^4\text{He}\mu)^+$ ion and a neutron. The rest of the notation is explained in Fig. 1.

and at tritium concentrations $c_t \approx 0.5$ the yield of reaction (1) (the number of neutrons generated by a single muon) is equal to

$$\nu = \frac{(\lambda_0 + \lambda_{dt}) \lambda_{dt\mu} c_d c_t}{\lambda_0 (\lambda_0 + \lambda_{dt} c_t + \lambda_{dt\mu} c_d^2)} \quad (4)$$

and the temporal distribution of neutrons from reaction (1a) is

$$\frac{dY_n}{dt} = \frac{\lambda_{dt\mu} c_d c_t}{\lambda_{dt} c_t + \lambda_{dt\mu} c_d^2} \{ \lambda_{dt} e^{-\lambda_1 t} + c_d (\lambda_{dt\mu} c_d - \lambda_{dt}) e^{-\lambda_2 t} \}, \quad (5)$$

where $\lambda_1 \approx \lambda_0$, $\lambda_2 \approx \lambda_0 + \lambda_{dt} c_t + \lambda_{dt\mu} c_d^2$.

Expressions (4) and (5) are valid for the theoretically predicted large values of λ_{dt} and $\lambda_{dt\mu}$:

$$\lambda_{dt\mu} c_d \gg \lambda_{tt\mu} c_t, \quad \lambda_{dt} c_t \gg \lambda_{dd\mu} c_d$$

and small values of ω_s , ω_t , and ω_d :

$$\omega_s \lambda_{dt\mu} c_d; \quad \omega_t \lambda_{tt\mu} c_t; \quad \omega_d \lambda_{dd\mu} c_d \ll \lambda_0.$$

Under these conditions the yield and temporal distribution of neutrons from reaction (1) are determined by the two unknown quantities λ_{dt} and $\lambda_{dt\mu}$, which can be found by comparing the experimental data on the yield and temporal distribution of neutrons from reaction (1) with expressions (4) and (5).

THE EXPERIMENTAL METHOD

The experiment was carried out in a muon beam from the JINR synchrocyclotron. A meson duct was used to lead a beam of muons of initial momentum 130 MeV/c into a low-background laboratory, where the main part of the apparatus—the gas target with the gas-supply system and the detectors—was set up. A diagram of the arrangement of the target and detectors in the muon beam is shown in Fig. 2.

The muons were detected by monitor counters 1–3 (a plastic scintillator), slowed down in moderator 6, detected by counter 4, and then allowed to hit the target 8. The muons that were stopped in the target initiated the reaction (1). The neutrons produced by this reaction were detected by detectors N1–N4 placed around the target, and the μ -decay electrons were detected by detectors E1–E8 placed in pairs around the target.

The main experimental idea which permitted a significant decrease of the background of random coincidences and the background due to muon stoppings in the walls of the target was the successive detection, during the 10 μsec interval (time gate) after a muon entered the target, of first the neutron from reaction (1) and then the μ -decay electron, that is, the use of delayed muon-neutron-electron coincidences. (Delayed μ - γ - e coincidences were used in Ref. 17 to study the $p d \mu \rightarrow {}^3\text{He}\mu + \gamma$ reaction.) The stopping of a muon in the material of the target walls (iron) leads either to the nuclear capture of the muon with the emission of a neutron (no electron) or to the decay of the muon (no neutron). The use of the n - e coincidence criterion has thus made it possible to ensure a small background level for our experimental conditions, where the num-

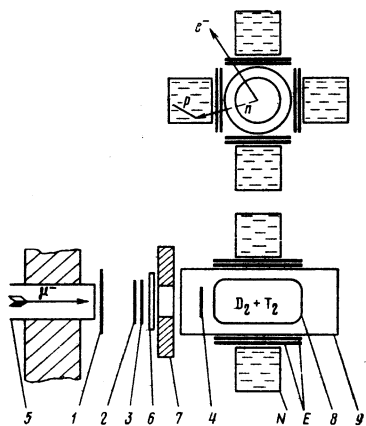


FIG. 2. The experimental setup: 1, 2, 3—monitor counters with plastic scintillators, 4—counter with CsI(Tl) crystal, 5, 7—collimators, 6—muon moderator, 8—gas target, 9—vacuum-tight housing, *N*—neutron detectors, *E*—electron detectors.

ber of muon stoppings in the target walls was a hundred times larger than in the gas. In addition, the level of background was also decreased by using counter 4 with a CsI(Tl) scintillator (100 mm diam \times 1 mm thick) located behind the moderator and directly in front of the target.

The main part of the experimental setup was the gaseous deuterium-tritium target.¹⁸ The following requirements were taken into account in its design: 1) a maximum pressure of 55 atm; 2) a range of working temperatures from -196 to 400 °C; 3) a sufficiently low level of gas release from the walls inside the working volume of the target ($<10^{-4}$ Torr/hr), which is necessary to maintain the purity of the gaseous $D_2 + T_2$ mixture at a level $<10^{-6}$ of the volume; 4) safety in working with large quantities of tritium (5000 Ci).

The target is sketched in Fig. 3. The body of the target is a stainless-steel cylindrical vessel 130 diam \times 250 mm. The volume of the target is 3.25 l and the wall thickness is 3 mm.

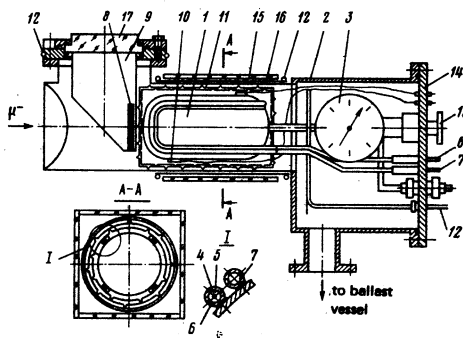


FIG. 3. Overall view of the gas target: 1—target, 2—vacuum-tight housing, 3—manometer, 4—heater, 5—ceramic beads, 6—copper heating tube, 7—tube for cooling the target with liquid nitrogen, 8—CsI(Tl) scintillator, 9—light-guide, 10—thermocouple, 11—heat screen, 12—tube for water cooling, 13—bellows valve, 14—flange of the vacuum-tight housing, 15—scintillators of the electron detectors, 16—copper screen, 17—Plexiglas light-guide.

As a safety precaution, the target itself and the manometer 3 and valve 13 connected to it were enclosed in a vacuum-tight housing connected to a ballast vessel. The combined volume of the housing and the vessel, which was 130 l, was large enough so that upon accidental breaking of the target seal the overall pressure of the gas mixture inside the vessel did not exceed 0.6 atm. The stem of the valve 13 was led out of the vacuum-tight housing through a seal on the flange 14. The CsI(Tl) crystal of the counter 8 with a hollow light-guide 9 was also located inside the housing.

The target was heated by a wire coil 4 passing through a copper tube 6 which was soldered to the body of the target and was cooled by blowing nitrogen gas through the copper tube 7, which also was soldered to the body of the target. The temperature of the target was measured by two thermocouples 10. The accuracy of the temperature measurements was $\pm 3^\circ$.

Since the scintillator 8 of the counter 4 was located inside the vacuum-tight housing and the scintillators 15 of the detectors *E1*–*E8* were located close together around the housing, it was necessary to reduce the heat transfer from the target to a minimum. For this purpose the exterior surface of the body of the target was polished and the target was surrounded by a four-layer screen 11 made of polished corrugated foils 80 μ m thick (made of stainless steel). In addition, the heat from the walls of the vacuum-tight housing and the light-guide of the counter 4 was removed by means of an external copper screen which was cooled by running water.

The target was filled with superpure deuterium and tritium using the gas supply system described in Ref. 19, a simplified diagram of which is given in Fig. 4. The required degree of purity of the hydrogen isotopes used was determined by the relation between the known values⁸ of the rate of transfer (λ_Z) of a muon from a hydrogen mesoatom to nuclei (*Z*) of the possible impurities (N_2 , O_2 , CO_2) and the expected values of $\lambda_{d\mu}$ and $\lambda_{t\mu}$. In order to keep the background due to transfer to the impurities to less than 1% it was necessary to satisfy the conditions $\lambda_Z c_Z / \lambda_{d\mu} c_d < 0.01$ and $\lambda_Z c_Z / \lambda_{t\mu} c_t < 0.01$, where c_Z is the relative impurity content. Using the values $\lambda_Z^0 = \lambda_Z / \varphi = 5 \times 10^{10} \text{ sec}^{-1}$, $\lambda_{d\mu}^0 = 10^8 \text{ sec}^{-1}$, and $\lambda_{t\mu}^0 = 3 \times 10^8 \text{ sec}^{-1}$, we find the condition

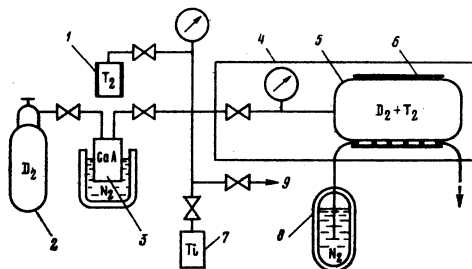


FIG. 4. Diagram of filling the target with deuterium and tritium: 1—ampoule with tritium, 2—vessel containing deuterium, 3—deuterium purification system using CaA zeolite adsorbers, 4—vacuum-tight housing, 5—gas target, 6—heater, 7—adsorber for the $D_2 + T_2$ mixture, 8—cooling system, 9—exit to the high-vacuum pumping system.

The deuterium was purified directly during the filling of the target by means of three tandem connected zeolite adsorbers ZI1–ZI3 placed in liquid nitrogen. The tritium source was titanium tritide TiT_2 placed inside an ampoule of stainless steel of volume 100 cm^3 . The dissociation of TiT_2 , that is, the generation of gaseous tritium, effectively occurs at a temperature $750\text{--}800^\circ\text{C}$. It is important that at this temperature TiT_2 actively adsorbs gases of different chemical materials, including oxygen, nitrogen, and carbon oxides, as a result of which the residual contamination of the tritium by these materials is less than 10^{-5} (Ref. 19). The relative content of tritium in our experiments did not exceed 10%, so that the tritium purity satisfied condition (6).

It was necessary not only to purify the deuterium and tritium before filling the target, but also to ensure that their purity was maintained at the required level (10^{-6}) during lengthy exposures (200 hours), that is, to eliminate contamination of the gas by release of other gases from the target walls and communication apparatus. For this purpose we carried out vacuum-thermal conditioning of the target and the communications apparatus; this was done during the 3 days before the target was filled. In order to control the parameters of the gas supply system we filled the target several times with the deuterium and then checked its purity. The results of these analyses indicated that the purity of the gas was better than 2×10^{-7} .

The target was first filled with tritium. The amount of tritium in the target was determined from the known target volume and the partial pressure of the tritium, measured with a compound pressure and vacuum gauge. The maximum tritium pressure at a TiT_2 temperature of 800°C was 480 Torr. The accuracy of determining the tritium content in the target was better than 1%. After the target was filled with tritium, the tritium was absorbed from the supply lines by titanium and then the target was filled with deuterium to the required pressure. Upon completion of a measurement run, the $D_2 + T_2$ mixture in the target was absorbed in Ti1 and Ti2 adsorbers filled with TNT-4 titanium. The adsorption capacity of each adsorber was 360 l under normal conditions. The residual pressure of the gas in the target and the communication apparatus after absorption of the mixture was no more than 10^{-3} Torr.

The scintillation detectors E1–E8 were used to register the electrons from the decay of the muons stopped in the target. These detectors were made of a plastic scintillator of dimensions $340 \times 200 \times 10\text{ mm}$ and FEU-30 photoelectron multipliers. The power supply dividers were arranged according to the scheme proposed in Ref. 20. In order to decrease the background of random coincidences, the electron detectors were connected pairwise for coincidence, forming four telescopes. The geometrical efficiency of all the detectors for the electrons emitted from the region of the target was 60%.

Neutrons from reaction (1) were recorded by four high-efficiency detectors N1–N4 with a NE-213 liquid

scintillator. The neutron recording system was described in Ref. 21. We used in the neutron detectors $100\text{ mm dia} \times 95\text{ mm}$ teflon windowless cells and a photomultiplier tube of the 58 AVP type (with photocathode diameter 110 mm). The cells were clamped directly to the entrance window of the photomultiplier without any intermediate transparent media. The use of this type of construction for the detector made it possible to improve the amplitude resolution by a factor of one-and-a-half compared to that for the neutron detectors usually employed with glass cells.

A simplified block diagram of the electronics is shown in Fig. 5. The "Master" block for selecting useful events transmitted signals from the E and N detectors to the time-to-code (T-C) and charge-to-code (C-C) converters during a $10\text{-}\mu\text{sec}$ gates triggered by a pulse from a coincidence of the signals from detectors 2 and 3. In order to suppress the "instantaneous" background from muon stoppings in the scintillators of the N and E detectors and in the walls of the target, we used "fast" (100 nsec) anticoincidences $23(\Sigma E + \Sigma N)$. The efficiency of selecting "neutron" events was increased by introducing "fast" anticoincidences (NE).

In order to discriminate between the background and the photons registered by the N detectors, we carried out $n\text{-}\gamma$ separation according to the shape of the scintillator pulse. For this we used an analog switching block as (Ref. 21); signals from an N detector entered this block and then at its exit two signals were formed whose amplitudes were proportional to the intensity of the fast (FC) and slow (SC) components of the scintillator pulse. The neutrons and photons were separated by analyzing the amplitudes of the FC and SC signals.

The information on an event, including the times of appearance of the signals from the N and E detectors (t_n and t_e), the amplitudes of the FC and SC signals (A_{FC} and A_{SC}), and the detector number (logic register LR) were sent for analysis to a computer when certain conditions were satisfied. We required that there be signals from the E and N detectors during the entire duration of the time gates and a signal from counter 4 during the $0.4\text{ }\mu\text{sec}$ from the instant that the gates were

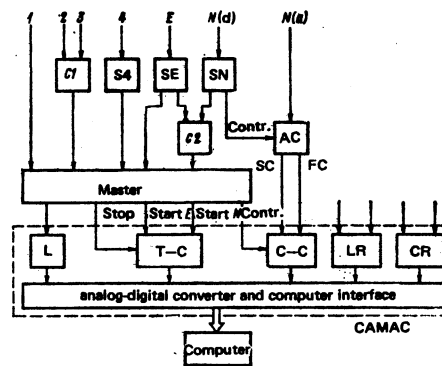


FIG. 5. The electronics: C1, C2—coincidence schemes, S4, SE, SN—shapers, N(a), N(d)—outputs to the anode and dinode of the neutron detector PM tubes, AC— analog switching block, Master—event selection block, J-C—time-to-code converters, C-C—charge-to-code converters, LR—logic register, CR—counting registers, L—LAM grader.

triggered, and also that there be no signal from counter 1 (a second muon) in an interval of duration $5 \mu\text{sec}$ prior to the opening of the time gates and $10 \mu\text{sec}$ after the opening of the gates. The monitor counts N_{23} and N_{234} were sent to the counting registers CR. Information from them was periodically sent to the computer.

Altogether we made 14 exposures in the muon beam with different temperatures of the $D_2 + T_2$ mixture or different deuterium and tritium contents. The conditions for each exposure are given in Table II. In exposures 1–4 the target was heated to $T = 613 \text{ K}$ and in exposures 9–14 it was cooled to 93 K . Exposures 1 and 6 differ in tritium content (by a factor of two) but have the same deuterium content and exposures 5 and 6 have different deuterium contents (by a factor of two) for the same tritium content. These conditions were chosen in order to determine how the yield of neutrons from reaction (1) changes when only $\lambda_{dt}^0 \varphi C_d$ or only $\lambda_{dt}^0 \varphi C_t$ is changed. Exposure 7 (pure deuterium) was carried out for an independent determination of the neutron background, and exposure 8 (vacuum) was carried out to find the electron background.

In each exposure we measured the temporal and amplitude characteristics of the events registered by the N and E detectors. As an example, in Fig. 6 we give the two-dimensional amplitude distribution (A_{FC} , A_{SC}) constructed for one of the neutron detectors according to the results of exposure 14. During the experiment we periodically carried out calibration measurements of the energy scale of the neutron detectors using standard ^{60}Co and Po-Be sources. The "neutron" exposures, in which events were selected in the regime of "fast" (100 nsec) anticoincidences ($N\bar{E}$) were periodically alternated with "electron" exposures, in which only the presence of a pulse from the E detectors was required.

ANALYSIS OF THE EXPERIMENTAL DATA

Preliminary processing of the experimental data was done directly in the course of a measurement run and consisted of separating the neutron and electron events and of constructing the temporal and amplitude distributions separately for each class of events. The electron events were those recorded in the electron exposures. The neutron events were taken to be those recorded in the neutron exposures and which belonged to the neutron region in the two-dimensional distribu-

TABLE II. Basic experimental data characterizing the exposures

Exposure	Gas pressure in the target at 293 K	Gas composition	Elemental tritium concentration C_t	Target temperature T , K	Number of recorded neutrons N_n	Number of recorded electrons $N_e \times 10^{-3}$
1	21.0 atm	$D_2 + T_2$	$3 \cdot 10^{-2}$	293	2762	566.1
2	" "	" "	" "	443	1996	384.3
3	" "	" "	" "	563	2003	382.5
4	" "	" "	" "	613	2107	407.6
5	10.5 "	" "	" "	293	1452	696.9
6	21.0 "	" "	$1.57 \cdot 10^{-2}$	293	1250	467.6
7	21.0 "	D_2	0	293	152	297.3
8	10^{-4} mm Hg	vacuum	0	293	24	42.9
9	6.6 atm	$D_2 + T_2$	$7.8 \cdot 10^{-2}$	93	98	52.0
10	" "	" "	" "	143	236	129.3
11	" "	" "	" "	193	207	93.6
12	" "	" "	" "	243	472	240.3
13	" "	" "	" "	293	273	135.9
14	66.2 "	" "	$0.81 \cdot 10^{-2}$	93	8765	1734.5

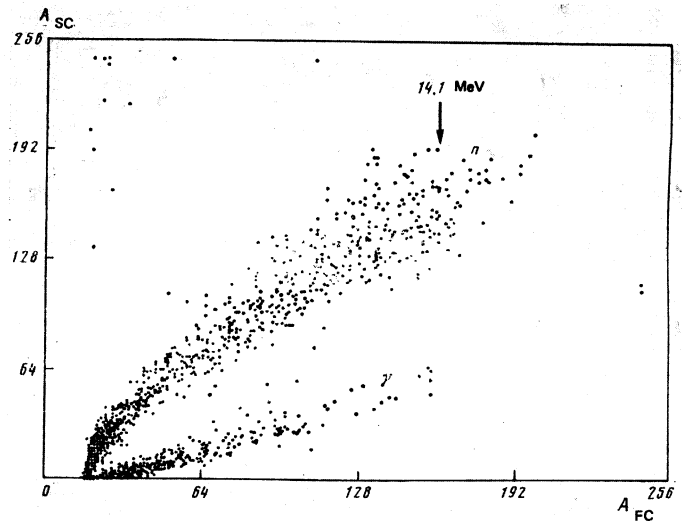


FIG. 6. Two-dimensional amplitude distribution of events recorded by one of the neutron detectors in exposure 14.

tions (A_{FC} , A_{SC}). In selecting "neutron" events for the purpose of suppressing the background from the fusion reaction $dd\mu \rightarrow {}^3\text{He} + n + \mu$ (neutron energy $E_n = 2.5 \text{ MeV}$) we used the criterion $E_n > 3 \text{ MeV}$. In addition, to discriminate between the background of random coincidences and the background from muons stopped in the target walls we required that there be an electron after the neutron during the $10 \mu\text{sec}$ time gate ($t_e > t_n$). The numbers of neutron (N_n) and normalized electron (N_e) events for exposures 1–14 are given in Table II.

In Fig. 7 we give the temporal neutron distribution summed over all the N detectors for exposure 6, and in Fig. 8 we give the amplitude distribution (the instrumental spectrum of the recoil protons) for one of the N detectors. The energy scale was calibrated according to measurements with ^{60}Co and Po-Be sources (the limits of the Compton-electron spectra are 0.98, 1.12, and 4.19 MeV, respectively) and the changeover from the electron energy E_e to the proton energy E_p was accomplished using the known limit of the recoil proton spectrum (14.1 MeV) for neutrons from reaction (1) and the relations between E_e and E_p obtained in Ref. 22.

In Fig. 9 we can see a clear temporal correlation between the registration times of a neutron from reac-

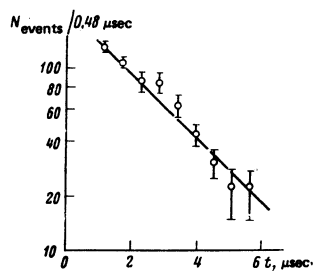


FIG. 7. Temporal distribution of neutron events registered in exposure 6. The axis of abscissas is the neutron detection time relative to the instant the muon hit the target and the axis of ordinates is the number of events per $0.48 \mu\text{sec}$ interval.

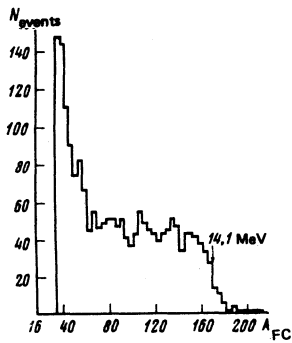


FIG. 8. Instrumental spectrum of recoil protons for neutrons of energy 14.1 MeV from reaction (1), recorded by one of the neutron detectors. The axis of abscissas is the amplitude of the FC signal (channels) and the recoil proton energy in MeV and the axis of ordinates is the number of events.

tion (1) and an electron from the decay of the muon that initiated this reaction.

In the first stage of the analysis we compared the relative values of the experimental neutron yield $Y'_n = N_n/N_e$ found in the different exposures. The following facts were established. First, the relative neutron yield does not change in a wide range of temperatures $T = 293-613$ K (the exposure run 1-5) and $T = 93-293$ K (exposures 9-13). The dependence of the neutron yield on the temperature of the $D_2 + T_2$ mixture is shown in Fig. 10.

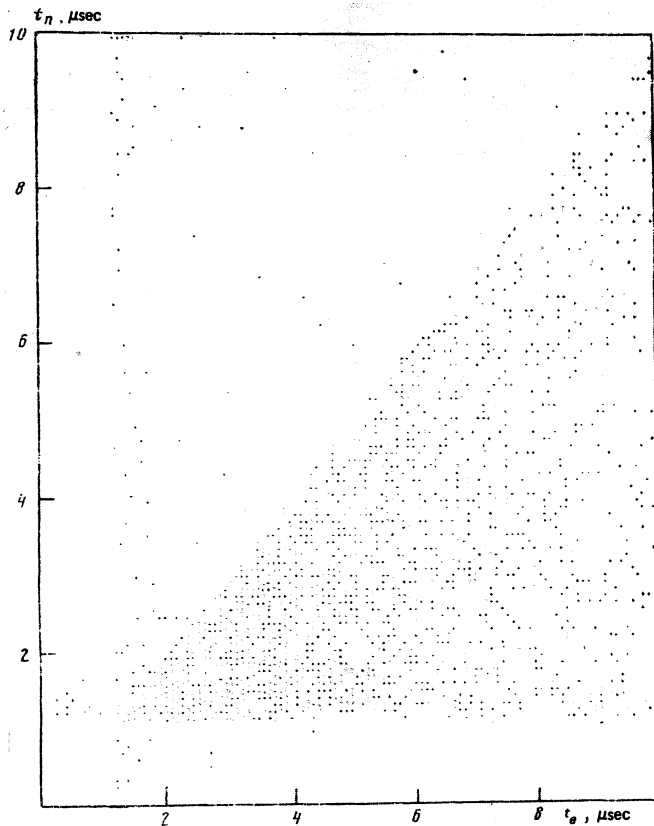


FIG. 9. Two-dimensional distribution of events from reaction (1). The abscissa is the time of recording the electron from μ decay and the ordinate the time of recording the neutron from μ catalysis (1).

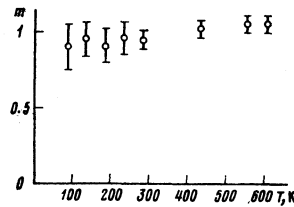


FIG. 10. Relative yield of neutrons from reaction (1) as a function of the temperature of the gaseous $D_2 + T_2$ mixture.

Secondly, the value of Y'_n practically does not change when only the deuterium content (φ_{D_2}) in the target is varied (according to the data from exposures 5 and 6). Conversely, when only the tritium content (φ_{T_2}) is varied in the $D_2 + T_2$ mixture (exposures 1 and 6) the neutron yield varies roughly proportionally to the value of φ_{T_2} . It follows from the form of expression (2) that these regularities in the variation of the neutron yield can be attributed to the fact that under our experimental conditions

$$\lambda_{d\mu}\varphi_{D_2} \gg \lambda_0, \quad \lambda_{dt}\varphi_{T_2} \leq \lambda_0.$$

Therefore, even at this stage of the analysis we have established a qualitative agreement between our experimental data and the theoretical predictions.^{5,11}

The nature of the neutron temporal distributions obtained in the various exposures is also in agreement with the theoretically predicted¹⁶ expression (5). Each such distribution can be written as the sum of two exponentials, the argument of one of them close to $\lambda_0 t$ and that of the other close to $\lambda_1 t$, where $\lambda_1 \gg \lambda_0$.

The complete analysis consisted of using the method of least squares to compare the experimental data on the neutron yield and temporal distributions obtained in each exposure with the theoretically expected expressions. The neutron yield was approximated as

$$Y'_n = N_n/N_e = \varepsilon_n Y_n(\lambda_{d\mu}, \lambda_{dt}), \quad (7)$$

where Y_n is the absolute neutron yield given by formula (4) and ε_n is the neutron-recording efficiency.

The value of ε_n was found by a calculation (using the Monte Carlo method) as in Ref. 23. In determining this quantity we took into account the interaction of the neutrons not only with the detector scintillators but also with all the other intermediate media in the path from the point of emission from the target to the scintillator (the target housing, and detector walls and the elements of the heating and cooling systems). In studying the interactions of neutrons with the material of the NE-213 scintillator we took into account both single and double scattering by hydrogen and carbon nuclei. In the calculation of ε_n we obtained the instrumental spectrum of the recoil protons with account taken of the real value of the energy resolution of the N detectors. An efficiency decrease due to the introduction of a threshold was found from the ratio of the number of events with $E_n > 3$ MeV to the total number of events in the spectrum. The value of ε_n found was 0.0110 ± 0.0012 .

The neutron temporal distribution was approximated by the relation

$$dY_n'/dt = Af(\lambda_{dt\mu}, \lambda_{dt}; t) + B, \quad (8)$$

where the function f is defined in (5), A is the normalization constant, and B is the background of random coincidences. The normalization condition was

$$\int_{t_1}^{t_2} (Af+B) dt = N_n,$$

where $t_1 = 0.1 \mu\text{sec}$ and $t_2 = 10 \mu\text{sec}$ are the beginning and the end of the measurement interval. In the course of analyzing the neutron temporal distributions we made use for control purposes, of a processing variant in which the argument of the first exponential in formula (5) was not fixed as $\lambda_1 = \lambda_0$, but assumed unknown. Then we obtained the value $\lambda_1 = (4.62 \pm 0.14) \times 10^5 \text{ sec}^{-1}$, which is in agreement with the known value $\lambda_0 = 4.55 \times 10^5 \text{ sec}^{-1}$.

RESULTS AND CONCLUSIONS

The optimal values of $\lambda_{dt\mu}^0$ and λ_{dt}^0 found in the analysis are

$$\lambda_{dt\mu} > 10^6 \text{ sec}^{-1} \quad (9)$$

(90% confidence level) and

$$\lambda_{dt}^0 = (2.9 \pm 0.4) \cdot 10^6 \text{ sec}^{-1}. \quad (10)$$

The error in λ_{dt}^0 is determined by the statistics of the useful and the background events and also by the errors in the calculations of ϵ_n . The experimental value (10) is in agreement with the value calculated in Ref. 10.

As can be seen from (9), we have obtained only a lower estimate for $\lambda_{dt\mu}^0$. This is explained by the fact that the yield of neutrons from reaction (1) [see expression (4)] is not very sensitive to the value of $\lambda_{dt\mu}^0$ at values $\lambda_{dt\mu}^0 \varphi C_d \gg \lambda_0$.

The limit (9) that we have obtained for $\lambda_{dt\mu}^0$ considerably exceeds the known production rates of other muonic molecules ($pp\mu$, $pd\mu$, and $dd\mu$) and is in agreement with the calculations of Ref. 5, carried out on the basis of a study of a resonance mechanism of mesomolecule production. The existence of this mechanism, established earlier for the $dd\mu$ molecule, is thereby also confirmed for the $dt\mu$ molecule.

According to the scheme of resonant $dt\mu$ production, we can expect a significant variation of the yield of neutrons from the fusion reaction (1) as a function of the $t\mu$ atom energy, that is, as a function of the temperature of the gaseous $D_2 + T_2$ mixture. We recall that for $dd\mu$ molecules the yield of the fusion reaction changes by roughly an order of magnitude in the deuterium temperature range $T = 120\text{--}380 \text{ K}$ (Refs. 2 and 3). However, as seen from Fig. 10, the yield of neutrons from reaction (1) is practically independent of the temperature of the $D_2 + T_2$ mixture in the range $T = 93\text{--}613 \text{ K}$. There can be two explanations for this.

The first is that in the entire range of temperatures that we studied the value of $\lambda_{dt\mu}$, varying with temperature as a function the resonance nevertheless stays large enough so that even at its minimum value in this range ($\lambda_{dt\mu}^{\text{min}}$) the condition $\lambda_{dt\mu}^{\text{min}} \gg \lambda_0$ holds. In this case, as follows from the form of expression (4), the neutron yield varies insignificantly with temperature.

Another possible explanation¹⁾ is that the mean lifetime of $t\mu$ atoms is mainly determined by $\lambda_{dt\mu}^0 \varphi C_d$ and under our conditions is $\leq 5 \times 10^{-7} \text{ sec}$, that is, smaller than the time necessary for thermalization from the initial energy 19 eV to thermal energies. It must be emphasized that in both cases the value of $\lambda_{dt\mu}^0$ at the maximum of the $\lambda_{dt\mu}^0(\epsilon_{t\mu})$ resonance dependence can significantly exceed our estimate (9).

Comparison of our data and the theoretical predictions^{5,8} on the possibility of effective muon catalysis in a $D_2 + T_2$ mixture indicates that the two important conditions necessary for the realization of this possibility are satisfied—the quantities $\lambda_{dt\mu}^0$ and λ_{dt}^0 are sufficiently large. It is especially important to experimentally determine the value of ω_s . From this viewpoint it is necessary to carry out experiments both at low density of the $D_2 + T_2$ mixture (pressure $\sim 1 \text{ atm}$), where it is possible to directly determine ω_s , and at high density (a pressure of hundreds of atmospheres), that is, under conditions where a large multiplicity of neutrons from μ catalysis of the $d+t$ reaction is expected.

Finally, a comprehensive study of the problem of muon catalysis in a mixture of deuterium and tritium requires the determination of the production rate of the $tt\mu$ molecule, the probability ω_t for the muon to “stick” to the helium nucleus produced in the fusion reaction $t+t$, and also a number of other characteristics of the process.

The authors are grateful to S.S. Gershtein and L.I. Ponomarev for numerous fruitful discussions about the μ catalysis problem, to A.T. Vasilenko, V.M. Romanov, and V.G. Sazonov for their help in planning and building the apparatus, to G.M. Osetinskiĭ and A. I. Filippov for a discussion of the problems associated with building an apparatus with a tritium target, and to P.V. Bakarin, G.F. Isaev, M.M. Petrovskii, Sh.G. Shamutdinov, A. A. Borisova, and L. M. Starshina for their help in the study.

The authors are deeply grateful to A. A. Bochvar and A. S. Nikiforov for their participation in carrying out this experiment.

¹⁾P. F. Ermolov pointed out this possibility to us (see also Ref. 24).

¹⁾L. W. Alvarez, H. Bradner, F. S. Crawford *et al.*, Phys. Rev. 105, 1127 (1957).

²⁾V. P. Dzhelepov, P. F. Ermolov, V. I. Moskalev, and V. V. Fil'chenkov, Zh. Eksp. Teor. Fiz. 50, 1235 (1966) [Sov. Phys. JETP 23, 820 (1966)].

- ³V. M. Bystritskiĭ, V. P. Dzhelepov, V. I. Petrukhin, A. I. Rudenko, L. N. Somov, V. M. Suvorov, V. V. Fil'chenkov, G. Hemnitz, N. N. Khovanskiĭ, B. A. Khomenko, and D. Horvath, *Zh. Eksp. Teor. Fiz.* **76**, 460 (1979) [*Sov. Phys. JETP* **49**, 232 (1979)].
- ⁴É. A. Vesman, *ZhETF Pis. Red.* **5**, 113 (1967) [*JETP Lett.* **5**, 91 (1967)].
- ⁵S. I. Vinitiskiĭ, L. I. Ponomarev, I. V. Puzynin, T. P. Puzynina, L. N. Somov, and M. P. Faĭfman, *Zh. Eksp. Teor. Fiz.* **74**, 849 (1978) [*Sov. Phys. JETP* **47**, 444 (1979)].
- ⁶S. S. Gerstein and L. I. Ponomarev, *Phys. Lett.* **72B**, 80 (1977).
- ⁷Yu. V. Petrov, *Proceedings of the Fourteenth Winter School of the Leningrad Institute of Nuclear Physics*, 1979, p. 139.
- ⁸V. M. Bystritskiĭ, V. P. Dzhelepov, Z. V. Ershova *et al.*, *ZhETF Pis. Red.* **31**, 249 (1980) [*JETP Lett.* **31**, 228 (1980)].
- ⁹S. S. Gerstein and L. I. Ponomarev, in *Muon Physics*, vol. III, eds. V. Hughes and C. S. Wu, New York, Academic Press, 4, 1975.
- ¹⁰H. Anderhub, J. Bocklin, P. LeCoultré *et al.*, *SIN Newsletters*, No. 12, 32 (1979).
- ¹¹L. I. Ponomarev, *Proceedings of the Seventh International Conference on Atomic Physics*, August 17-22, 1978, Riga, Zinatne and Plenum Press, p. 182.
- ¹²Ya. B. Zel'dovich and A. D. Sakharov, *Zh. Eksp. Teor. Fiz.* **32**, 947 (1957) [*Sov. Phys. JETP* **5**, 775 (1957)]; J. D. Jackson, *Phys. Rev.* **106**, 330 (1957).
- ¹³S. S. Gershteĭn, Yu. V. Petrov, L. I. Ponomarev, N. P. Popov, L. P. Presnyakov, and L. N. Somov, *Zh. Eksp. Teor. Fiz.* **80**, 1690 (1981) [*Sov. Phys. JETP* **53**, (1981)].
- ¹⁴L. I. Ponomarev and M. P. Faĭfman, *Zh. Eksp. Teor. Fiz.* **71**, 1689 (1976) [*Sov. Phys. JETP* **44**, 886 (1977)].
- ¹⁵Ya. B. Zel'dovich and S. S. Gershteĭn, *Usp. Fiz. Nauk* **71**, 581 (1960) [*Sov. Phys. Uspekhi* **3**, 593 (1961)].
- ¹⁶S. S. Gershteĭn, Yu. V. Petrov, L. I. Ponomarev, L. N. Somov, and M. P. Faĭfman, *Zh. Eksp. Teor. Fiz.* **78**, 2099 (1980) [*Sov. Phys. JETP* **51**, 1053 (1980)].
- ¹⁷E. J. Bleser, E. W. Anderson, L. M. Lederman, S. L. Meyer, J. L. Rosen, J. E. Rothberg, and I.-T. Wang, *Phys. Rev.* **132**, 2679 (1963).
- ¹⁸V. M. Bystritskiĭ, V. K. Kapyshev, S. Sh. Mukhamet-Galeeva, L. A. Rivkis, V. I. Satarov, and V. A. Stolupin, *JINR R13-80-288*, Dubna, 1980.
- ¹⁹V. M. Bystritskiĭ, V. P. Dzhelepov, V. G. Zinov, V. M. Romanov, V. I. Satarov, V. A. Stolupin, and Sh. G. Sham-sutdinov, *JINR R13-80-825*, Dubna, 1980.
- ²⁰V. S. Nadezhdin, *JINR R13-10833*, Dubna, 1977.
- ²¹V. G. Zinov, V. S. Nadezhdin, A. I. Rudenko, L. N. Somov, and V. V. Fil'chenkov, *JINR R13-80-32*, Dubna, 1980.
- ²²V. V. Verbinski, W. R. Burrus *et al.*, *Nucl. Instr. Meth.* **65**, 8 (1968).
- ²³V. M. Bystritskiĭ, L. S. Vertogradov, and V. V. Fil'chenkov, *JINR 1-7527*, Dubna, 1973.
- ²⁴J. Rafelsky, *Exotic Atoms*, '79 Ettore Majorana School 177-205, Plenum Press, New York, 1980.

Translated by Patricia Millard